Cathepsin B causes trogocytosis-mediated CAR T cell dysfunction

Kenneth A. Dietze[1], Kiet Nguyen[2], Aashli Pathni[3], Frank Fazekas[2], Jillian M. Baker[1], Etse Gebru[4], Alexander Wang[1], Wenxiang Sun[5], Ethan Rosati[5], David Lum[5], Aaron P. Rapoport[4], Xiaoxuan Fan[4], Djordje Atanackovic[4], Arpita Upadhyaya[2,6,7], Tim Luetkens[1,4]

[1] Department of Microbiology and Immunology, University of Maryland School of Medicine, Baltimore, MD, USA

[2] Biophysics Graduate Program, University of Maryland, College Park, MD, USA

[3] Biological Sciences Graduate Program, University of Maryland, College Park, MD, USA

[4] Department of Medicine and Transplant/Cell Therapy Program, University of Maryland School of Medicine and Marlene and Stewart Greenebaum

[5] Preclinical Research Resource, Huntsman Cancer Institute, Salt Lake City, UT, USA

[6] Institute for Physical Science and Technology, University of Maryland, College Park, MD, USA

[7] Department of Physics, University of Maryland, College Park, MD, USA

One sentence summary: CAR-mediated trogocytosis is mediated by the cysteine protease cathepsin B and directly causes CAR T cell exhaustion and fratricide.

Word count (abstract): 210

Word count (main text): 3,829

Figures/Tables: 5 Figures, 5 Suppl. Figures, 1 Suppl. Table

*Corresponding author:
Tim Luetkens, M.D.
Associate Professor of Microbiology and Immunology
Director R&D at Fannie Angelos Cellular Therapeutics Laboratory
University of Maryland
655 W Baltimore St, RM. 9-009
Baltimore, MD 21201
Phone: 410-706-1924
Email: tluetkens@som.umaryland.edu

GRAPHICAL ABSTRACT

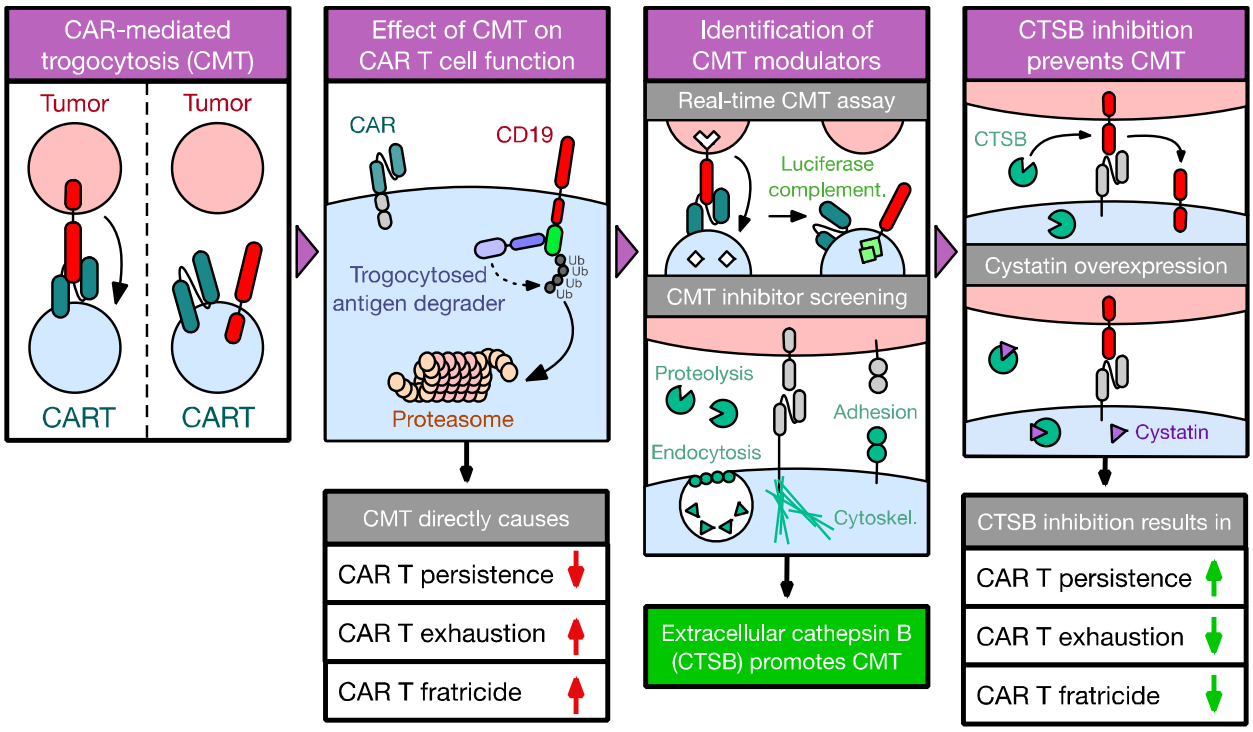

ABSTRACT

Chimeric antigen receptor (CAR) T cell therapy has shown remarkable efficacy in cancer treatment. Still, most patients receiving CAR T cells relapse within 5 years of treatment. CAR-mediated trogocytosis (CMT) is a potential tumor escape mechanism in which cell surface proteins transfer from tumor cells to CAR T cells. CMT results in the emergence of antigen-negative tumor cells, which can evade future CAR detection, and antigen-positive CAR T cells, which has been suggested to cause CAR T cell fratricide and exhaustion. Whether CMT indeed causes CAR T cell dysfunction and the molecular mechanisms conferring CMT remain unknown. Using a selective degrader of trogocytosed antigen in CAR T cells, we show that the presence of trogocytosed antigen on the CAR T cell surface directly causes CAR T cell fratricide and exhaustion.

By performing a small molecule screening using a custom high throughput CMT-screening assay, we found that the cysteine protease cathepsin B (CTSB) is essential for CMT and that inhibition of CTSB is sufficient to prevent CAR T cell fratricide and exhaustion. Our data demonstrate that it is feasible to separate CMT from cytotoxic activity and that CAR T cell persistence, a key factor associated with clinical CAR T cell efficacy, is directly linked to CTSB activity in CAR T cells.

INTRODUCTION

Chimeric antigen receptors (CAR) are genetically engineered proteins combining antigen binding domains with immune cell activation domains[1–3]. T cells and natural killer (NK) cells engineered to express CARs recognize tumor-associated antigens with high specificity and have been shown to be effective at targeting several hematologic malignancies[1,4–7]. It has previously been shown that CAR T cells and CAR NK cells rapidly transfer the targeted antigen from tumor cells to their own cell surface in a process called trogocytosis[8–10]. CAR-mediated trogocytosis (CMT) is associated with increased expression of apoptotic and exhaustion markers as well as reduced expansion[8–10]. In addition, it has been shown that T cells engineered to express the tumor antigen CD19 are efficiently killed by other CD19 CAR T cells ("fratricide")[8]. Mechanistically linking CMT to exhaustion, fratricide, and reduced CAR T cell expansion has, so far, been elusive due to the lack of specific inhibitors of trogocytosis.

In this study, we develop an analytical framework to investigate CMT and determine the effects of CMT on CAR T cell function as well as its mechanistic basis.

RESULTS

CAR T cells acquire target antigen via trogocytosis

CAR-mediated trogocytosis (CMT) is the extraction of the targeted tumor antigen from the tumor cell surface and its incorporation into the CAR T cell plasma membrane[8–11] (Fig. 1A). *Ex vivo*, CMT occurs across cancer types[8,9] and target antigens, including CD19, CD22[8], mesothelin[8], and BCMA[11]. We found robust transfer of CD19 to CD19-targeting CAR T cells (clone: FMC63) as well as CD19 loss on tumor cells (Fig. 1B/C), which can be observed just seconds after CAR T cells contact target cells (Fig. 1D, Suppl Fig. S1A). Similarly, we confirmed transfer of *B cell maturation antigen* (BCMA), the target of two clinically approved CAR T cell approaches for the treatment of multiple myeloma[4,5,12,13] (Fig. 1E) to BCMA CAR T cells (Fig. 1F) and loss of BCMA from tumor cells (Fig. 1G) independent of CAR format (Fig. 1E). In the clinical setting, CMT had only been shown to occur in B cell lymphoma patients treated with CAR NK cells[10]. By analyzing peripheral blood mononuclear cells (PBMCs) from patients who had recently received CD19 CAR T cells, we demonstrate that CMT also occurs in patients treated with CAR-expressing T cells (Fig. 1H/I).

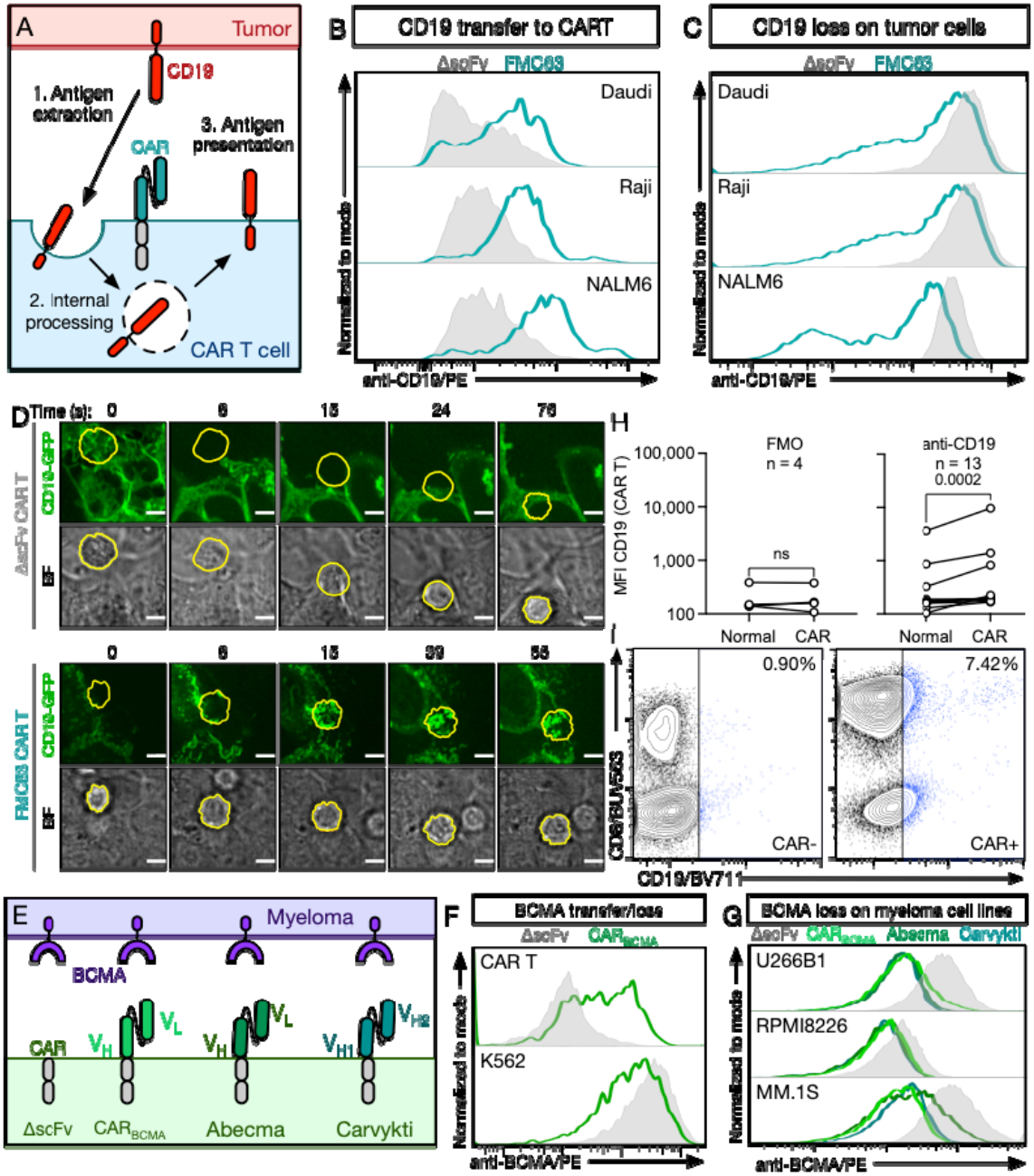

Figure 1: CD19 and BCMA CAR T cells rapidly acquire target antigen via trogocytosis. (A) Schema of CAR-mediated trogocytosis (CMT). **(B)** CD19 transfer to CAR T cells lacking an antigen binding domain (ΔscFv) or CD19 CAR T cells (FMC63) after a 1-hour coculture with CD19-positive cell lines at a 0.5:1 effector-target ratio using flow cytometry. **(C)** CD19 loss on tumor cells after a 1-hour coculture with ΔscFv or FMC63 CAR T cells at a 0.5:1 effector-target ratio using flow cytometry. **(D)** Observation of CMT in brightfield and confocal images of ΔscFv

or FMC63 CAR T cells cultured with CD19-GFP-expressing 293T cells. CD19 is shown in green. Scale bar represents 5µm. **(E)** Schema of different BCMA-targeting CAR T cells. **(F)** BCMA transfer to CAR T cells and BCMA loss on BCMA-GFP-expressing K562 cells after coculture with CAR_{BCMA} T cells. **(G)** BCMA loss on MM.1S, RPMI8226, and U266B1 cells when cocultured with CAR_{BCMA}, Abecma, and Carvykti CAR T cells. **(H-I)** Amount of CD19 on CAR T cells isolated from patients 7-28 days after receiving CD19 CAR T cell therapy using full-spectrum flow cytometry. Data indicate individual patients. Statistical significance was determined by Wilcoxon matched-pairs signed-rank test.

CAR-mediated trogocytosis directly causes CAR T cell dysfunction

The presence of trogocytosed antigen on CAR T cells is correlated with increased exhaustion and reduced viability[8–10] but it remains unknown if CMT is the cause of these effects. To answer this question, we developed an approach for the targeted degradation of trogocytosed CD19 fused to GFP (CD19-GFP) in CAR T cells (Fig. 2A). Expression of a trogocytosed antigen degrader (TAD), the E3-targeting domain Nslmb[14,15] fused to a GFP-binding protein (TAD_{GFP}), results in a significant reduction of total and surface CD19-GFP in 293T cells (Suppl Fig. S2A/B). Expression of TAD_{GFP} did not alter CAR T cell expansion during manufacturing or short-term antitumor activity (Suppl Fig. S2C/D).

When cocultured for 2 hours with K562 cells expressing CD19-GFP, conventional FMC63 CAR T cells showed increased levels of CD19 (Fig. 2B) and GFP (Fig. 2C) indicative of CMT. However, when co-expressing TAD_{GFP}, CD19 and GFP levels were significantly reduced in FMC63 CAR T cells after coculture. Targeted degradation of trogocytosed antigen was also validated using a fully human TAD (TAD_{CD19}) construct directly targeting CD19. TAD_{CD19} recognizes CD19 by using the Lyn kinase SH2 domain (Fig. 2E), which has been shown to bind the intracellular domain of CD19 with high affinity[16]. Similar to TAD_{GFP}-expressing CAR T cells, co-expression of TAD_{CD19} in FMC63 CAR T cells also resulted in reduced CMT (Fig. 2F/G). These data indicate that selective degradation of trogocytosed antigen is feasible in CAR T cells and that this approach can be used to explore the effects of CMT on CAR T cell function.

Using the TAD system, we next investigated the effect of CMT on CAR T cell fratricide. We found that TAD_{GFP} expression did not alter the proliferation of CAR T cells when co-

cultured with $CD19^+$ tumor cells (Suppl. Fig. S2E). However, TAD_{GFP} expression resulted in significantly increased CAR T cell numbers after co-culture (Fig. 2D), indicating that CMT directly causes CAR T cell death, likely due to fratricide.

It has previously been shown that FMC63 can bind CD19 in *cis*[17] and could thereby cause persistent CAR signaling followed by T cell exhaustion (Suppl. Fig. S2F). We found that FMC63 CAR T cells that had acquired CD19 during co-culture with CD19-GFP-expressing K562 cells showed increased expression of exhaustion markers TIM-3 and LAG-3 compared to negative control T cells expressing a CAR without a binding domain (ΔscFv, Fig. 2H/I). Expression of TAD_{GFP} prevented TIM-3/LAG-3 upregulation on these cells demonstrating that increased exhaustion marker expression is the direct consequence of trogocytic antigen transfer to CAR T cells (Fig. 2H/I). CMT-induced fratricide and exhaustion could substantially limit long-term CAR T cell anti-tumor activity. In a serial coculture stress test of CAR T cell efficacy (Fig. 2J), we found that TAD_{GFP} substantially increased the ability of CAR T cells to control B cell acute lymphoblastic leukemia (B-ALL, Fig. 2K).

These data demonstrate that CMT directly causes CAR T cell dysfunction and fratricide, and thereby limits CAR T cell expansion and anti-tumor activity.

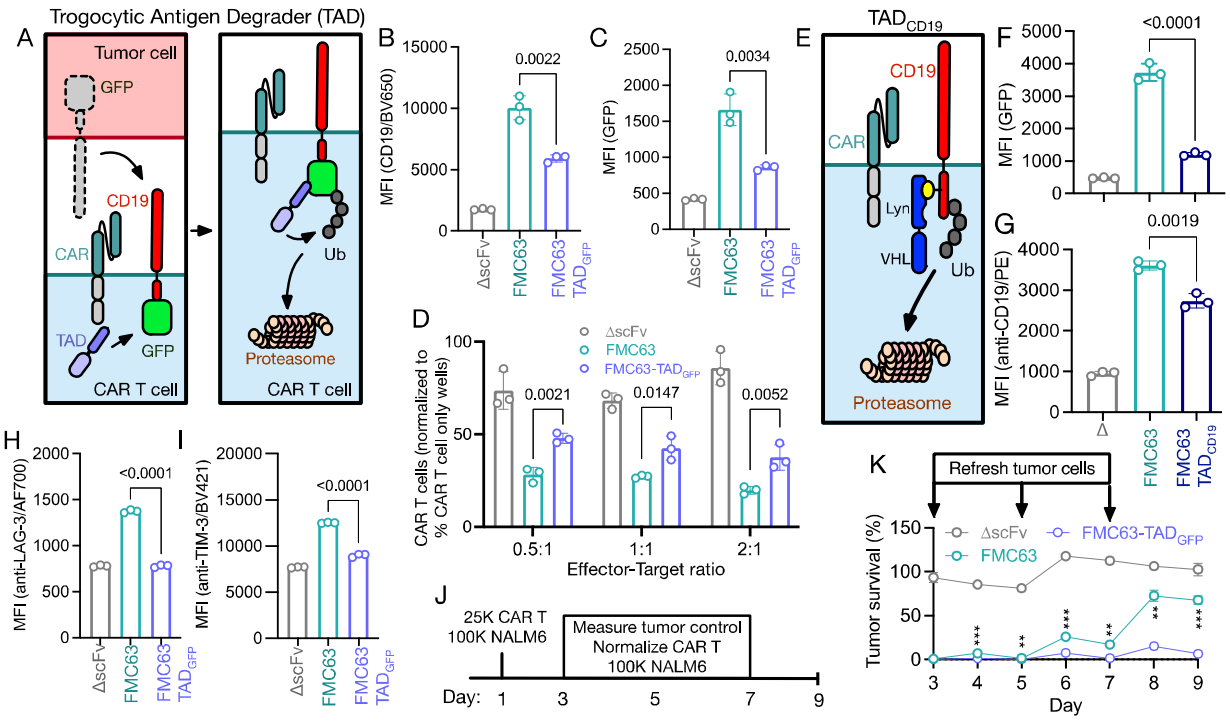

Figure 2: CAR-mediated trogocytosis directly causes CAR T cell dysfunction. (A) Schema of trogocytosed antigen degrader (TAD). **(B)** CD19 and **(C)** GFP expression on FMC63 CAR T cells expressing TAD_{GFP} or T cells expressing a CAR lacking a binding domain (ΔscFv) following a 1-hour coculture with CD19-GFP-expressing NALM6 cells as determined by flow cytometry. **(D)** Quantification of CAR T cells after a 24-hour coculture with CD19-GFP-expressing NALM6 cells using flow cytometry. Values are normalized to wells containing only CAR T cells. **(E)** Schema of a fully human-derived TAD system (TAD_{CD19}). VHL = von Hippel-Lindau protein; Ub = ubiquitin. **(F)** GFP and **(G)** CD19 expression on FMC63 CAR T cells expressing TAD_{CD19} or ΔscFv CAR T cells after a 1-hour coculture with CD19-GFP-expressing NALM6 cells at a 0.5:1 effector-target ratio. **(H)** Expression of LAG-3 and **(I)** TIM-3 on CAR T cells expressing TAD_{GFP} after a 24-hour coculture with CD19-GFP-expressing NALM6 cells using full-spectrum flow cytometry. (B-I) Statistical significance was determined by two-tailed Student's *t*-test. **(J)** Schema of *in vitro* serial coculture experiment to determine long-term CAR T cell expansion and antitumor activity. **(K)** Survival of CD19-GFP-expressing NALM6 cells expressing firefly

luciferase (Fluc) at a 0.5:1 effector-target ratio using a luminescence-based cytotoxicity assay. Data indicates mean ± S.D. from three technical replicates. Tumor survival was normalized to untreated tumor cells. Statistical significance was determined by multiple *t*-tests and corrected for multiple comparisons using the Bonferroni-Dunn method.

Real-time detection of CAR-mediated trogocytosis by luciferase complementation assay

Little is known regarding the molecular and cellular drivers of CMT, and to date there are no high-throughput assays to systematically probe potential modulators of CMT as it occurs in real-time. To address this, we developed a luciferase complementation assay for the real-time detection of CMT (CompLuc, Fig. 3A). In the CompLuc assay, luciferase complementation occurs following the transfer of CD19 fused to the C-terminal fragment of NanoLuc[18] (cLuc) to CAR T cells, which express the complementary cytosolic N-terminal NanoLuc (nLuc) fragment that has a high affinity for cLuc[18] (Fig. 3B, Suppl. Fig. S3A/B). The CompLuc assay allows for highly sensitive detection of small numbers of $nLuc^{+}cLuc^{+}$ CAR T cells in cocultures (Fig. 3C). We demonstrate that CMT, as quantified by CompLuc, is antigen- and CAR-dependent, and correlates with effector-target ratio (Fig. 3D-F) and flow cytometry endpoint analysis (Fig. 3D/F).

To validate the CompLuc assay, we determined the effect of an established modulator of CMT, the actin polymerization inhibitor cytochalasin D[8,19]. Treatment of CAR T cells with cytochalasin D significantly reduced CMT in a dose-dependent manner as measured by CompLuc assay (Fig. 2G), demonstrating the ability of the assay to identify modulators of CMT.

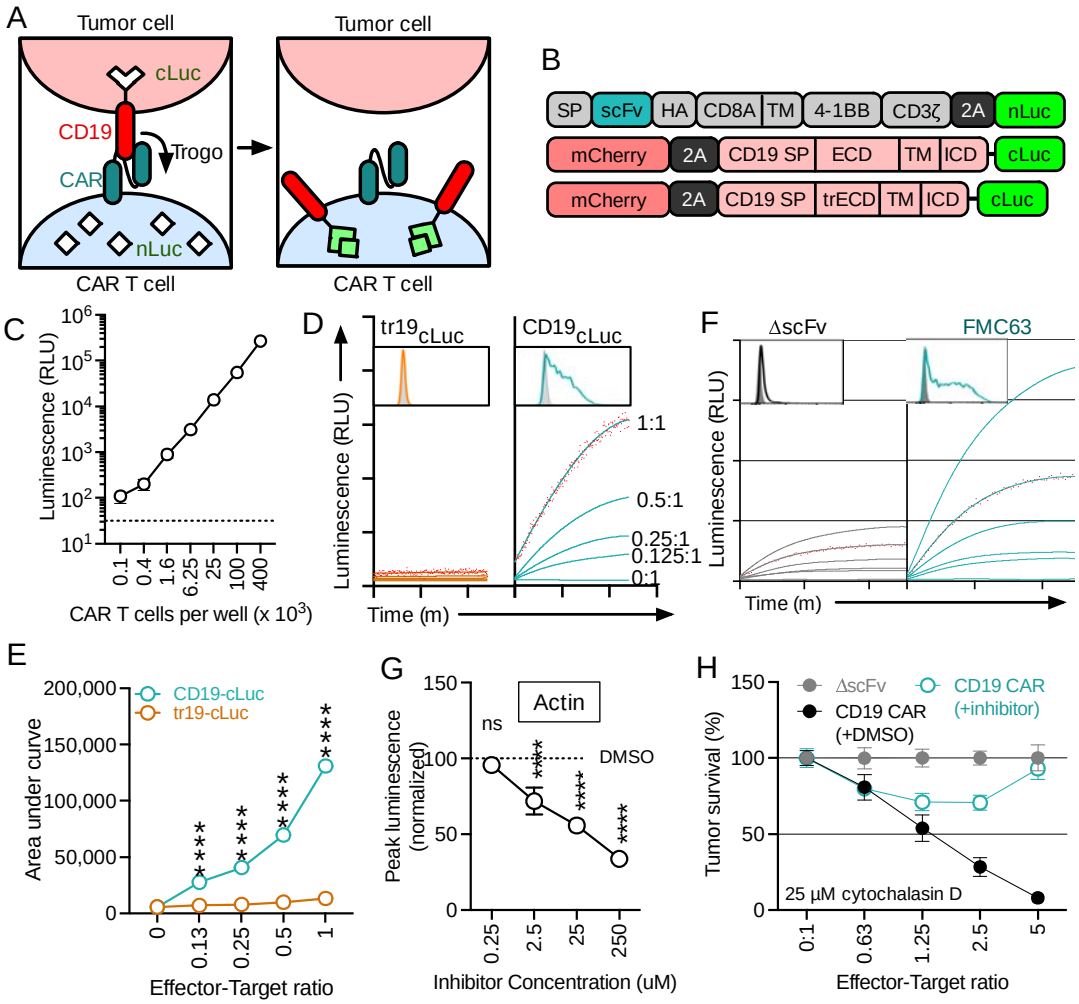

Figure 3: Luciferase complementation assay allows for the real-time detection of trogocytosis. (A) Schema of luciferase complementation assay (CompLuc). **(B)** Schema of constructs used for CAR T cells (I) and tumor cells (II/III) for development of luciferase complementation assay. SP = signal peptide; HA = hemagglutinin tag; TM = transmembrane region; ECD = extracellular domain; trECD = truncated extracellular domain; ICD = intracellular domain. **(C)** Luminescence of nLuc+cLuc+ CAR T cells. Data represent mean ± S.D. of three technical replicates. **(D)** CMT during coculture of FMC63 CAR T cells expressing nLuc with K562 cells expressing full length (teal) or truncated (tr19, orange) CD19 fused to cLuc using CompLuc or flow cytometry after 1 hour at the indicated effector-target ratios. CMT using CompLuc was measured for a total 2.5 hours at 1-minute intervals. Data represents best fit of

three technical replicates. **(E)** Area-under-curve quantification of luminescence in Fig. 2D. **(F)** CMT during coculture of ΔscFv or FMC63 CAR T cells expressing nLuc with K562 cells expressing full length CD19-cLuc using CompLuc or flow cytometry after 1 hour at the indicated effector-target ratios. CMT using CompLuc was measured for a total 2.5 hours at 1-minute intervals. Data represents best fit of three technical replicates. **(G)** Peak luminescence of FMC63 CAR T cells cocultured with K562 cells expressing CD19-cLuc at a 1:1 effector-target ratio as determined by CompLuc. CAR T cells were pre-treated with cytochalasin D for 1 hour at the indicated concentrations. **(H)** Survival of Raji-Fluc cells after 16-hour coculture with FMC63 CAR T cells pre-treated with the indicated concentrations of cytochalasin D. CMT values are normalized to a DMSO control. (G/H) Data represent mean ± S.D. of three technical replicates.

Extracellular cathepsin B is a key driver of CAR-mediated trogocytosis

CMT may be the result of incomplete target cell killing followed by the endocytosis of target cell fragments, as suggested by the simultaneous effect of cytochalasin D on CMT and CAR-mediated cytotoxicity (Fig. 3H). However, we hypothesized that, while the molecular mechanisms driving target cell killing and trogocytosis may overlap, CMT could in part be mechanistically distinct from cytotoxic function.

To identify functional systems that could be specifically involved in CMT but not cytotoxicity, we explored the effect of inhibiting various processes at the T cell immune synapse on CMT[8,19–22] (Fig. 4A). We found that inhibition of cathepsin B (CTSB) with the small molecule inhibitor Ca-074-Me in FMC63 CAR T cells reduced CMT in a dose-dependent manner as measured by CompLuc (Fig. 4B) without substantially altering CAR T cell cytotoxicity (Fig. 4C). Using a membrane-impermeable inhibitor of CTSB, we found that inhibition of extracellular CTSB alone is sufficient to prevent CMT (Fig. 4D).

CTSB is a ubiquitously expressed cysteine protease, primarily localized to lysosomal and endosomal compartments under physiological conditions, where it is primarily involved in protein degradation and turnover[23,24]. However, CTSB is also found in the cytosol and exocytic vesicles, retains its catalytic activity at neutral pH[25], and has been shown to line exocytic granules of cytotoxic T lymphocytes[26]. In addition to proteolytic degradation within the endosome and lysosome, CTSB has been implicated in the degradation and remodeling of components of the extracellular matrix, such as collagen and fibronectin, thereby promoting the invasion and metastasis of tumor cells[25,27,28]. Similarly, CTSB may contribute to the extraction of antigen-rich membrane fragments of target cells prior to their transfer to CAR T cells.

To further support the potential role of extracellular CTSB produced by CAR T cells in CMT, we next determined whether CTSB in CAR T cells is actively transported to the immune synapse upon antigen contact. To this end, we generated FMC63 CAR T cells expressing CTSB fused to mCherry and exposed these cells to immobilized CD19 (Fig. 4E). We found that CTSB in FMC63 CAR T cells but not in ΔscFv CAR T cells, rapidly localized to the immune synapse following CAR T cell antigen recognition (Fig. 4F-H, Suppl. Fig. S1A), correlating with increased CMT as measured by CompLuc and flow cytometry (Fig. 3F). These findings indicate that transport of CTSB to the immune synapse and its subsequent secretion by CAR T cells are necessary for CMT.

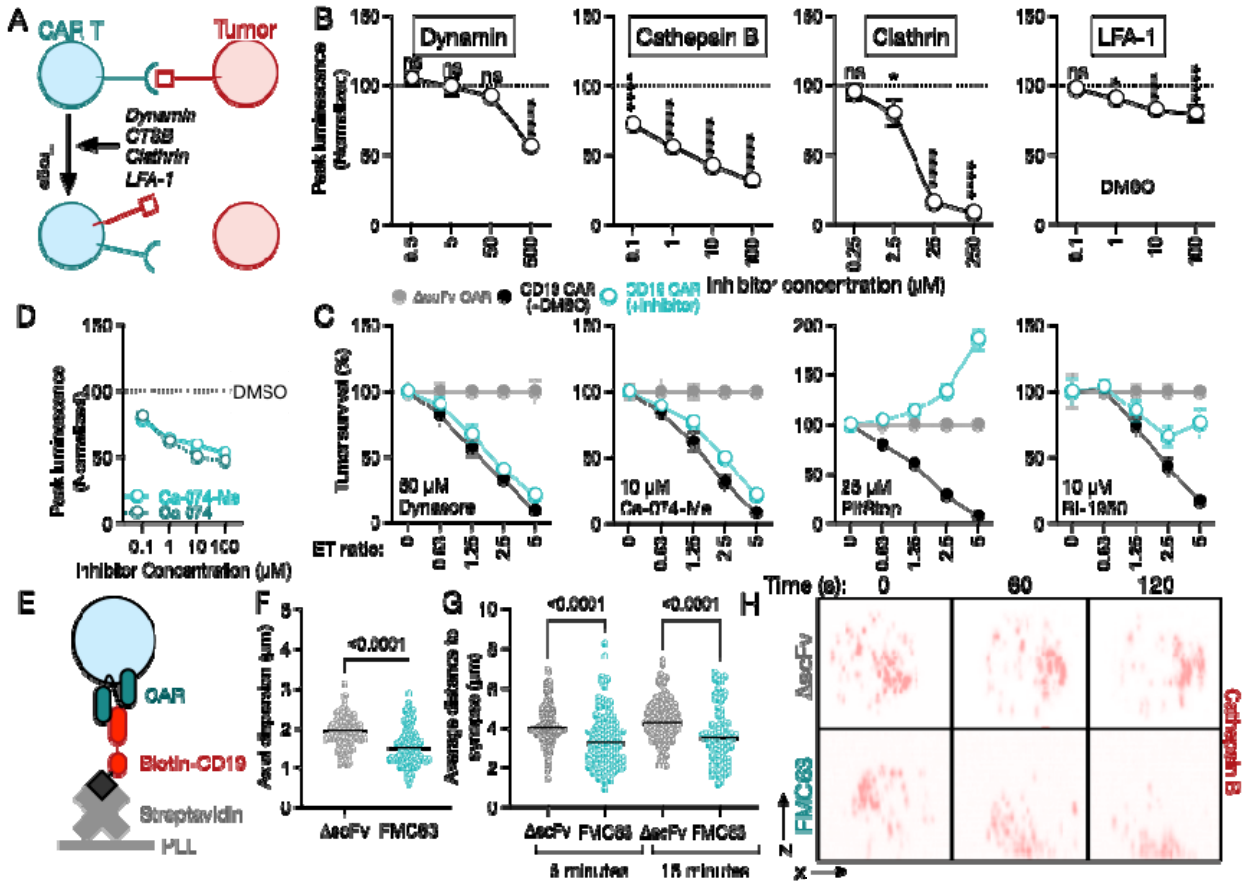

Figure 4: Extracellular cathepsin B is a key driver of CAR-mediated trogocytosis. (A) Schema of potential modulators of CMT. **(B)** Peak luminescence as determined by CompLuc of FMC63 CAR T cells treated with inhibitors of the indicated proteins cocultured with K562 cells expressing CD19-cLuc at a 1:1 effector-target ratio. Values are normalized to a DMSO control. **(C)** Survival of Raji-Fluc cells after 16-hour coculture with FMC63 CAR T cells treated with inhibitors of the indicated proteins at a single concentration. Tumor survival was measured using a luciferase-based cytotoxicity assay. **(D)** Peak luminescence as determined by CompLuc of FMC63 CAR T cells cocultured with K562 cells expressing CD19-cLuc at a 1:1 effector-target ratio. FMC63 CAR T cells were pre-treated with the indicated concentrations of Ca-074-Me (membrane permeable) or Ca-074 (membrane impermeable). Values are normalized to a DMSO control. (B-D) Data represent mean ± S.D. of three technical replicates. **(E)** Schema of microscopy setup used to assess cathepsin B (CTSB) localization to the immune synapse.

Biotinylated CD19 was immobilized on plate-bound NeutrAvidin. FMC63 CAR T cells expressing CTSB-mCherry were added to slides and imaged using confocal microscopy. **(F)** Axial dispersion of CTSB in fixed ΔscFv and FMC63 CAR T cells 5 minutes after plating. **(G)** Average distance of CTSB to immune synapse in fixed ΔscFv and FMC63 CAR T cells 5 minutes and 15 minutes after plating. (F/G) Statistical significance was determined by two-tailed Student's *t*-test. **(H)** Side (x-z) view of the distribution of CTSB-mCherry in ΔscFv or FMC63 CAR T cells on immobilized CD19 at indicated time points using spinning disk confocal imaging.

Cystatin abundance controls CTSB activity and CMT

CTSB is ubiquitously expressed across tissues and cell types and its activity is regulated through a network of endogenous protease inhibitors called cystatins[29]. Cystatin A (CSTA) has been described as the main regulator of CTSB activity[30] and, similar to Ca-074, CSTA inhibits CTSB through insertion of a hydrophobic wedge into the active-site cleft of CTSB[31] (Fig. 5A). To determine if CSTA abundance directly regulates CMT in CAR T cells, we engineered CAR T cells to stably overexpress CSTA (CAR_{CSTA}, Suppl. Fig. S4A). We confirmed that CSTA overexpression led to significantly increased amounts of CSTA protein in CAR T cells (Fig. 5B), which resulted in overall reduced CTSB activity (Fig. 5C) without altering in vitro expansion (Suppl. Fig. S4B/C) or CAR T cell phenotype (Suppl. Fig S4D/E). When co-cultured with tumor cells expressing the respective target antigens, CD19 CAR_{CSTA} cells showed equivalent anti-tumor activity compared to conventional CAR T cells (Fig. 5D, Suppl. Fig. S4F) whereas BCMA CAR_{CSTA} cells showed slightly improved short-term antitumor activity (Suppl. Fig. S4G). When co-cultured with $CD19^+$ or $BCMA^+$ tumor cells, we observed significantly reduced CMT in CAR_{CSTA} cells as measured by CompLuc (Fig. 5E/F, Suppl. Fig. S4H/I) despite comparable CAR T cell activation (Suppl. Fig. S5A). CMT was similarly reduced when overexpressing the closely related protein cystatin B[32] (Suppl. Fig S5B) or truncated $CSTA_{1\text{-}57}$ (Suppl. Fig S5C) containing the hydrophobic wedge (Suppl. Fig. S5D/E). Overexpression of cystatins reduced both antigen transfer to CAR T cells (Fig. 5G/H, Suppl. Fig. S5F) and antigen loss on tumor cells (Fig. 5I/J, Suppl. Fig. S5G), suggesting inhibition of CMT at the antigen extraction step. This CSTA-mediated inhibition of CMT resulted in significantly increased CD19 and BCMA CAR T cell

expansion when exposed to tumor cells in vitro (Fig. 5K/L, Suppl. Fig. S5H) and in vivo (Suppl. Fig. S5I/J), further demonstrating that inhibition of CMT improves CAR T cell persistence.

Taken together, these data demonstrate that CTSB expressed in CAR T cells is rapidly transported to the immune synapse upon antigen stimulation and, following secretion, confers extraction of target antigen from tumor cells and subsequent transfer to CAR T cells. The abundance of the endogenous CTSB inhibitor CSTA in CAR T cells efficiently controls CMT, with high CSTA abundance significantly prolonging in vitro and in vivo CAR T cell expansion/persistence.

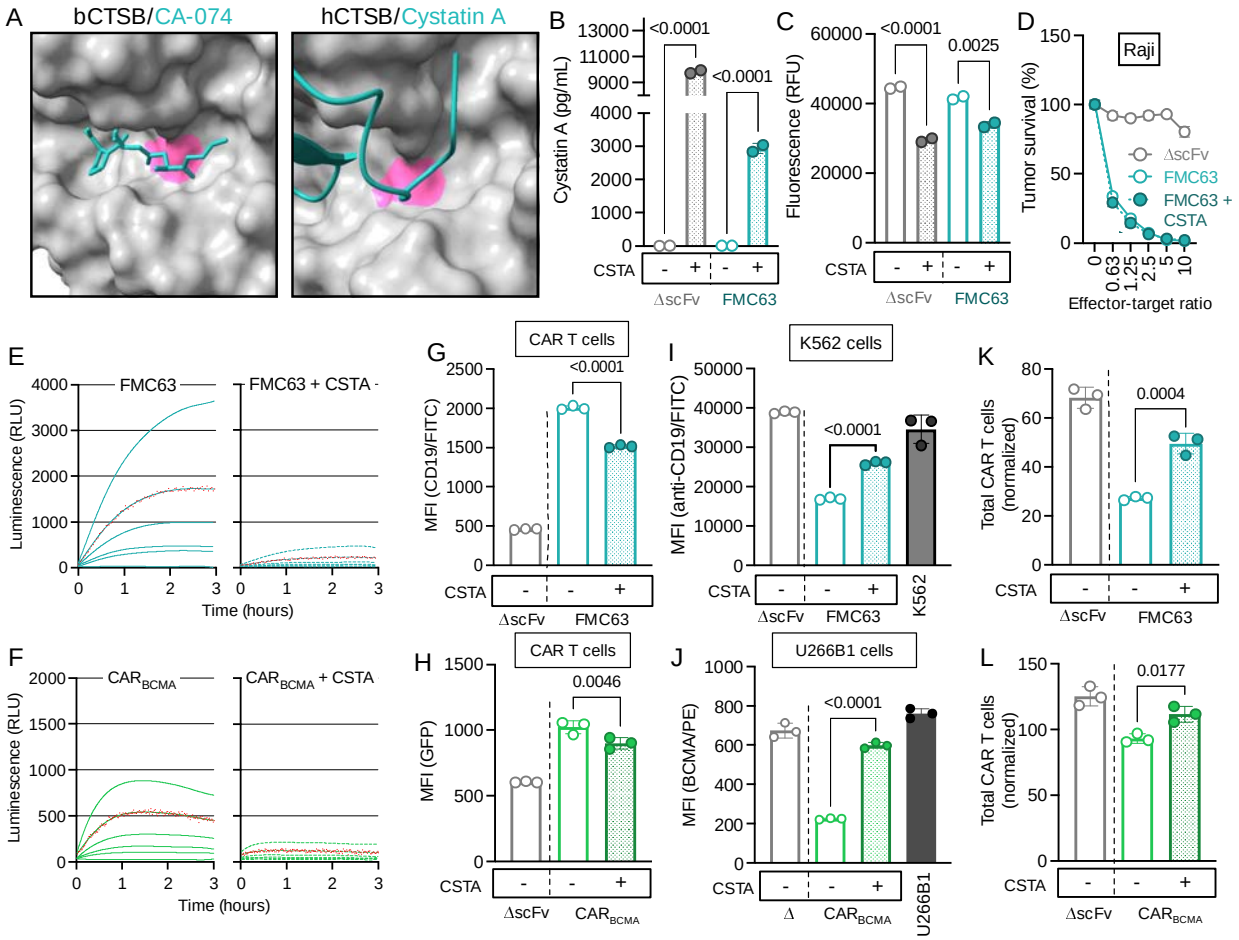

Figure 5: Cystatin abundance controls CTSB activity and CMT. (A) Crystal structures of bovine cathepsin B in complex with Ca-074 (left, PDB: 1QDQ) and human cathepsin B in complex with cystatin A (right, PDB: 3K9M). The active site cysteine of cathepsin B is shown in pink; Ca-074 and cystatin A are shown in teal. **(B)** Levels of CSTA in CAR or CAR_{CSTA} T cells measured by ELISA. **(C)** Cathepsin B activity in CAR or CAR_{CSTA} T cells measured by fluorescence. (J/K) Data represent mean ± S.D. of two technical replicates. Statistical significance was determined by two-tailed Student's *t*-test**. (D)** Survival of Raji-Fluc cells after a 16-hour coculture with FMC63 CAR or CAR_{CSTA} T cells at the indicated effector-target ratios. Data represent mean ± S.D. of three technical replicates. **(E)** CMT of FMC63 CAR or CAR_{CSTA} T cells as determined by CompLuc using K562 cells expressing CD19-cLuc after 3 hours. **(F)** CMT of BCMA CAR or CAR_{CSTA} T cells as determined by CompLuc using K562 cells expressing

BCMA-GFP-cLuc after 3 hours. (E/F) Data represents best fit of three technical replicates. **(G)** CD19 transfer to CAR T cells following a 30-minute coculture of FMC63 CAR or CAR_{CSTA} T cells and K562 cells expressing CD19-cLuc at a 0.5:1 effector-target ratio. **(H)** BCMA-GFP transfer to CAR T cells following a 2-hour coculture of BCMA CAR or CAR_{CSTA} T cells and K562 cells expressing BCMA-GFP-cLuc at a 1:1 effector-target ratio. **(I)** CD19 loss on tumor cells following a 30-minute coculture of FMC63 CAR or CAR_{CSTA} T cells and K562 cells expressing CD19-cLuc at a 0.5:1 effector-target ratio. **(J)** BCMA loss on U266B1 tumor cells following a 2-hour coculture of BCMA CAR or CAR_{CSTA} T cells and K562 cells expressing BCMA-GFP-cLuc at a 1:1 effector-target ratio. **(K)** Total CAR T cells following a 30-minute coculture of FMC63 CAR or CAR_{CSTA} T cells and K562 cells expressing CD19-cLuc at a 0.5:1 effector-target ratio. **(L)** total CAR T cells following a 2-hour coculture of BCMA CAR or CAR_{CSTA} T cells and K562 cells expressing BCMA-GFP-cLuc at a 1:1 effector-target ratio. (K/L) CAR T cell numbers are normalized to wells containing only CAR T cells using counting beads. (G-L) Statistical significance was determined by two-tailed Student's *t*-test.

DISCUSSION

CAR T cells have revolutionized cancer immunotherapy, but most patients receiving CAR T cell therapy relapse within 5 years of treatment[33–35]. Several mechanisms driving relapse after CAR T cell therapy have been described, including CAR T cell-mediated trogocytosis (CMT). We demonstrate that CMT affects CAR T cell function in three key ways: 1) by rendering tumor cells temporarily antigen negative, 2) by causing CAR T cells to be killed by other CAR T cells, and 3) by inducing CAR T cell exhaustion, potentially through persistent cis signaling[36]. Previous studies had demonstrated the presence of tumor antigen on CAR T cells following co-culture with tumor cells and that the presence of trogocytosed antigen was correlated with increased apoptotic markers and exhaustion[8–10]. However, it had remained unknown if this T cell dysfunction was caused by CMT.

In this study, using targeted degradation of trogocytosed antigen-GFP fusion proteins, we now demonstrate that CMT directly causes CAR T cell fratricide and exhaustion. We also demonstrate that the trogocytosed antigen degrader (TAD) approach can be adapted to degrade endogenous antigens by using endogenous protein domains binding to the target antigen's intracellular domain. Further work will be needed to explore target specificity/orthogonality of such endogenous binding domains to ensure CAR T cell functionality.

To determine if CMT is mechanistically distinct from cytotoxic CAR T cell function, we developed a high-throughput luciferase complementation screening assay for the kinetic assessment of CMT to determine the effect of a set of small molecule inhibitors. In this screen, we found that the cysteine protease cathepsin B (CTSB) produced by CAR T

cells is essential for CMT but dispensable for tumor cell killing. We subsequently demonstrated that CTSB produced by CAR T cells rapidly localizes to the immune synapse upon antigen stimulation and that extracellular CTSB produced by CAR T cells confers antigen extraction from tumor cells. A predominant role of extracellular CTSB in the processing of cellular material is in line with prior studies describing the involvement of CTSB in the degradation and remodeling of components of the extracellular matrix[25,27,28]. We further show that CTSB activity in CAR T cells is tightly regulated through the abundance of cystatins, a class of endogenous protease inhibitors[29,31]. We found that overexpression of both cystatin A and cystatin B potently inhibited CTSB in CAR T cells. While the small molecule inhibitors used throughout this study have been shown to be specific for CTSB[37,38], the more robust inhibition of CMT by cystatins, which are able to inhibit a range of cathepsins, including cathepsin L and H, could indicate a role of other cathepsins in CMT[29,31]. Future work will be needed to further delineate the precise molecular mechanism by which extracellular CTSB and potentially other cathepsins are able to confer antigen extraction from tumor cells without causing tumor cell death.

Our study focused on approaches targeting the two clinically validated CAR T cell antigens CD19 and BCMA approved for the treatment of several hematologic malignancies. However, we propose that future work should also include an in-depth exploration of CMT in solid malignancies. In this setting, exhaustion-driven T cell dysfunction is generally more pronounced[39,40] and CMT may play a key role. In addition, a denser tumor microenvironment and constrained T cell mobility may favor more extensive intratumoral fratricide.

In conclusion, we show that CTSB is essential for CMT and that CMT directly causes CAR-mediated fratricide and exhaustion. CTSB activity is controlled by the abundance of endogenous human cystatins and cystatin overexpression results in significantly reduced CMT, fratricide, exhaustion and increased CAR T cell persistence. Our findings provide evidence that CMT is mechanistically distinct from cytotoxic function in CAR T cells and support the rational targeting of this resistance mechanism in CAR T cells.

MATERIALS AND METHODS

Study approval

All recombinant DNA and biosafety work was approved by the institutional biosafety committees at University of Maryland, Baltimore (protocol IBC-6040). Animal experiments were approved by the institutional animal care and use committee at the University of Utah (protocol 18-1104).

Cell lines and primary human cells

Raji, NALM6, Daudi, DB, Toledo, MM.1S, RPMI8226, U266B1, K562, and Phoenix-AMPHO cells were purchased from the American Type Culture Collection (ATCC) and cultured according to ATCC instructions. Lenti-X 293T cells were purchased from Takara and cultured according to the manufacturer's instructions. Cell lines were authenticated by their respective supplier. Healthy donor buffy coats were obtained from the New York Blood Center. PBMCs from healthy donors were isolated from buffy coats by density gradient using FillPaque (GE) as previously described[13,41]. Primary human T cells were cultured in AIM-V medium (Invitrogen 12055-083) supplemented with 5% Human serum (Sigma H4522-100ML), 1% Pen/Strep (Thermofisher 15140-122) (T cell media), and 40 IU IL-2 (R&D Systems #202-IL-10). All cells were cultured at 37°C, 5% CO2.

Vector constructs

All vectors generated for this study were produced by Twist Biosciences. FMC63-nLuc contains the CD19-specific scFv fragment FMC63 [43]. All CAR constructs contain the CD8α hinge/transmembrane domain, 4-1BB costimulatory domain, and CD3z domain.

For some constructs, the full-length sequence of human cystatin A (UniProt, P01040) was synthesized and cloned downstream of the respective CAR and nLuc fragment separated by a P2A sequence (Twist Bioscience). DNA was isolated using Endofree Plasmid Maxi Kit (Qiagen 12362) following the manufacturer's protocol. Plasmid concentration was measured using a NanoDrop One instrument (Thermo). All DNA constructs were stored at -20°C.

Clinical data

Whole blood was drawn from patients receiving CAR T cell therapy 7-28 days after CAR T cell injection. Peripheral blood mononuclear cells (PBMCs) were isolated by density gradient using Ficoll Paque as previously described[13,41]. PBMCs were stained with anti-hCD3, anti-hCD4, anti-hCD8, anti-CAR, and anti-hCD19, anti-hCD27, anti-hCD137, and 7-AAD and analyzed by flow cytometry. Samples were collected under Institutional Review Board (IRB)-approved protocol 2043GCCC (IRB H0091736, PI D. Atanackovic).

Gamma retrovirus Production

Gammaretrovirus was produced using Phoenix-AMPHO cells (ATCC, catalog no. CRL-3213). Phoenix-AMPHO cells were transiently transfected with 16 µg of plasmid DNA using Opti-MEM Reduced Serum Medium (Thermofisher, catalog no. 31985070) and lipofectamine 2000 (Invitrogen 11668-019) according to manufacturer's instructions. During transfection, cells were cultured in Dulbecco's Modified Eagle Medium (DMEM, Thermofisher 11995073) supplemented with 10% FBS. Virus-containing supernatant was filtered using Steriflip™ Sterile Disposable Vacuum Filter Units (Millipore Sigma SEIM003M00). Virus was concentrated using Retro-X Concentrator (Takara, 631456). The following day, concentrated virus was centrifuged at 1500 x g for 45 minutes at 4°C.

Supernatant was removed and concentrated virus was resuspended in 1.5 mL complete T cell media.

Transgenic T cell production and expansion

CAR T cells were generated as previously described[11,34,42]. Buffy coats from healthy donors were obtained from the New York Blood Center and peripheral blood mononuclear cells (PBMCs) were isolated using Ficoll-Paque and cryopreserved until use. PBMCs were thawed and cultured overnight in complete T cell media. PBMCs were stimulated for 2 days with anti-CD3/anti-CD28 T cell activation beads (Thermo, catalog no. 11131D) in the presence of interleukin-2 (IL-2; 40 IU/ml; R&D Systems, catalog no. 202-IL-010) in complete T cell media and incubated at 37°C, 5% CO_2. Bead-stimulated cells were transferred to RetroNectin-coated (Takara) virus–containing plates and incubated overnight. Transduction was repeated the next day before counting and diluting cells to 0.4×10^6 cells/ml. After the second transduction, cells were grown for an additional 7 days before removing beads using a DynaMag-15 magnet (Thermo Fisher Scientific). IL-2 was replenished every 2 days to 40 IU/ml. Cells were frozen in 90% fetal bovine serum/10% dimethyl sulfoxide and stored in liquid nitrogen. CAR T cell transduction efficiency and phenotype were determined by flow cytometry. CAR T cells were washed with FACS buffer and stained with antibodies targeting hCD3, HA, hCD4, hCD8, hCD95, hCD62L, and hCD45RA.

Imaging Substrate Preparation

Eight-well chambers (Cellvis, catalog no. C8-1.5H-N) were used for all experiments. For CAR T cell activation on CD19-coated surfaces, 8-well chambers were coated with 0.01% poly-L-lysine (PLL) solution diluted in distilled water for 10 minutes at room

temperature. PLL was aspirated from each well, and the chambers were allowed to air-dry for 1 hour at 37°C. PLL-coated dishes were then incubated overnight at 4°C with a 10 µg/mL solution of NeutrAvidin (Thermo Scientific, catalog no. 31000) in 1x Dulbecco's phosphate-buffered saline (DPBS). After overnight incubation, coated wells were washed with 1x DPBS at room temperature and incubated at 37°C with a 10 µg/mL solution of biotinylated human CD19 protein (ACRO Biosystems catalog no. CD9-H82E9) in DPBS for 2 hours at 37°C. Prior to the experiment, coated wells were washed three times with RPMI 1640 phenol red-free imaging medium. For coculture experiments, 8-well chambers wells were incubated with 10 µg/mL fibronectin (MilliporeSigma, catalog no. 34-163-11MG) in DPBS at room temperature for 1 hour prior to seeding with 293T cells stably expressing CD19-GFP. 293T cells were seeded at a concentration of 5 x 10^5 cells per well in complete growth media, followed by an overnight incubation at 37°C, 5% CO_2. Prior to imaging, wells were washed three times with warm complete imaging media, consisting of a 1:1 ratio of RPMI 1640 supplemented with 5% fetal bovine serum (FBS) and DMEM supplemented with 10% FBS. The washing process was performed thrice to ensure removal of any residual media while leaving a known volume in the wells.

Confocal Microscopy

Confocal microscopy was conducted using an inverted microscope (Nikon Ti-E PFS, Nikon Inc.) equipped with a 100× Silicone objective lens. Imaging was performed with a Prime BSI camera (Photometrics). Image acquisition protocols were managed using Nikon Elements software, and images were cropped in FIJI for further analysis. All live cell imaging was done with imaging chambers placed in a stage-top Okolab Incubator

(Okolab S. R. L.) pre-equilibrated to 37°C with 5% CO_2. For live cell imaging on glass, activated CAR T cells suspended in RPMI 1640 medium supplemented with 5% FBS were deposited onto CD19-coated surfaces. Imaging was started between 3 to 6 minutes after CAR T cells expressing CTSB-mCherry were added to a biotin-CD19-coated coverslip. For each well, timelapse images of a 3D volume (planes with z spacing of 0.3 µm to span the cell from the top to the bottom) were acquired every 3 minutes for 60 minutes. For coculture experiments, imaging was started between 3 to 6 minutes after CAR T cells expressing CTSB-mCherry were dropped onto a layer of 293T cells expressing CD19-GFP seeded on a coverslip, at a concentration of 7×10^4 cells per drop. Brightfield imaging was used to identify cells attached to the apical surface of HEK293 cells. The synaptic plane between a CAR-T cell and a HEK293 cell was identified and designated as the home plane for acquisition of Z-stack time-lapse movies. Two-channel images using 488 nm and 561 nm lasers (for GFP and mCherry imaging respectively) were acquired every 3 minutes for 1 hour and 15 minutes utilizing a Z-spacing of 0.3 or 0.6 µm, with brightfield images taken at the home plane.

Image analysis was carried out in MATLAB (Mathworks, Inc.) using custom scripts. The plane of the synapse was determined using the actin channel. After background subtraction, axial intensity gradients are estimated for every voxel of sufficient intensity within the ROI. Below the cell, these gradients are typically positive due to the Airy pattern of the PSF. The synapse is taken as the first plane for which the gradients are no longer consistently positive.

Estimating the average distance of CTSB to the synapse

The center of fluorescence (COF) of CTSB is defined similarly to the center of mass. The voxel positions are weighted by CTSB intensity after background subtraction and thresholding to obtain the COF. The average CTSB distance is then calculated from the axial (z) distance of the Cathepsin B COF to the plane of the synapse.

Characterizing CTSB axial dispersion

The axial dispersion is an estimate of the average distance of CTSB molecules to the COF. The axial (z) distance of each voxel to the COF is determined, and the axial dispersion is defined as the average of these distances weighted by CTSB intensity after background subtraction and thresholding. Voxels with sufficiently low signal do not contribute to the calculation due to the thresholding procedure.

CTSB clustering at the synapse

The pair auto-correlation function g(r) of CTSB is computed at the synapse using the actin channel as a mask[44]. The actin channel is segmented by smoothing with a Gaussian filter, generating an initial mask by applying k-means clustering (k = 2) after a log transformation, and then applying morphological operations to connect and smooth the initial mask. The clustering coefficient, g_{ave}, is computed by averaging over all radial bins with 0.25 m or 0.5 m.

CompLuc-based trogocytosis assay

Transduced, cryopreserved nLuc+ CAR T cells were thawed and cultured in complete T cell media supplemented with 40 IU IL-2 for 48 hours prior to use. nLuc-expressing CAR T cells were cocultured with CD19-cLuc-expressing K562 tumor cells at the specified effector-target ratios. CAR T cells and tumor cells were resuspended in Opti-MEM

reduced serum media. Live Cell Substrate (Promega, catalog no. N2011) was prepared according to manufacturer's instructions. K562 tumor cells and prepared Live Cell Substrate were added to wells of a black 96-well plate and luminescence was measured to assess baseline luminescence. CAR T cells were added to appropriate wells and luminescence was measured every minute for three hours at 37˚C. Luminescence was measured using a Spark multi-mode plate reader (Tecan).

Flow cytometry-based trogocytosis assay

A flow-cytometry based trogocytosis assay was used to confirm results observed in CompLuc, to assess CD19 levels on CAR T cells and tumor cells, and to quantify CAR T cells. 2 x 10^5 target cells were seeded in wells of a 96-well round bottom plate. Various ratios of CAR T cells were cocultured with target cells for 1 hour at 37˚C, 5% CO_2. Following coculture, cells were resuspended by gentle pipetting and transferred to wells of a 96-well V bottom plate for washing and staining. Cells were stained with Zombie violet fixable viability dye, and antibodies for hCD3, HA, and hCD19. Accucheck counting beads (Life Technologies) were added to the cells. Samples were acquired on an LSR II flow cytometer (BD) or an Aurora full-spectrum flow cytometer (Cytek).

Luciferase-based cytotoxicity assay

To determine *in vitro* CAR T cell cytotoxicity, cell lines (Raji, NALM6, Daudi, Toledo) were transduced with pHIV-Luc-ZsGreen lentivirus and sorted on a FACS Aria flow cytometer (BD) for GFP expression. 3 x 10^4 target cells were seeded in wells of a 96-well round bottom plate. CAR T cells were cocultured with target cells at the indicated effector-target ratios and incubated for 16 hours at 37˚C, 5% CO_2. Following incubation, 80 µL of supernatant was harvested from each well. Cells were suspended by gentle

pipetting, and 100 µL was transferred to a 96-well black flat bottom plate. D-Luciferin (Gold Biotechnology, catalog no. LUCNA-2G) at 150 µg/ml was added to the cells and incubated for 5 minutes at 37°C. Luminescence was determined on a Spark multimode plate reader (Tecan).

Serial coculture repeat stimulation assay

To determine the long-term *in vitro* control and exhaustion of CAR T cells, luciferase-expressing tumor cells were plated at 3 x 10^4 cells/well. CAR T cells were cocultured at a defined effector-target ratio and incubated for 24 hours at 37˚C, 5% CO_2. Following incubation, cells were transferred to a 96-well black flat bottom plate. D-luciferin was added to cells and luminescence was determined on a Spark multimode plate reader (Tecan). Next, remaining CAR cells were pooled together and normalized based on expansion. CAR T cells were redistributed to wells and fresh tumor cells were added to each well. Plates were incubated for 48 hours at 37˚C, 5% CO_2. Luminescence measurements and normalization were repeated until a loss of cytotoxicity was observed.

Cystatin A enzyme-linked immunosorbent assay

Cystatin A concentration was assessed using a Human Cystatin A ELISA kit (Invitrogen, catalog no. EH140RB). Total cell lysates were extracted from CAR T cells using radioimmunoprecipitation assay (RIPA) buffer (Thermo) containing protease inhibitor cocktail (Roche). Total protein concentration was determined using Pierce BCA assay (Thermo). Cystatin A levels were determined by enzyme-linked immunosorbent assay (ELISA) according to manufacturer's instructions (Invitrogen) and calculated using

standard curve interpolation. Absorbance was measured at the recommended wavelength on a Spark multimode plate reader (Tecan).

Cathepsin B activity assay

Cathepsin B activity was assessed using the InnoZyme Cathepsin B Activity Assay Kit (MilliPore Sigma, catalog no. CBA001). Total cell lysates were extracted from CAR T cells using the provided cell lysis buffer according to manufacturer's instructions. Total protein concentration was determined using Pierce BCA assay (Thermo Fisher Scientific). Cathepsin B activity was determined fluorometrically according to manufacturer's instructions (Calbiochem). Fluorescence was measured on a Spark multimode plate reader (Tecan).

Treatment of CAR T cells with inhibitors

FMC63 CAR T cells were treated with small-molecule inhibitors targeting Actin (inhibitor: Cytochalasin D, Sigma Aldrich catalog no. C8273), Dynamin (inhibitor: DynaSore, Sigma Aldrich catalog no. D7693), Cathepsin B (inhibitor: Ca-074-Me, SelleckChem catalog no. S7420), Clathrin (inhibitor: PitStop, Abcam catalog no. ab120687), or LFA-1 (inhibitor: BI-1950, Boehringer Ingelheim) at the indicated concentrations for one hour. Following treatment, cells were washed with T cell media and centrifuged at 400 x g for 5 minutes. To determine the effect of the non-membrane permeable CTSB inhibitor CA-074 (Millipore Sigma, catalog no. 205530), the inhibitor was added directly to the co-culture at the indicated concentrations. As a control, CAR T cells treated with DMSO. CAR T cells were cocultured with CD19-expressing tumor cells for the indicated intervals.

Western blot

Total cell lysates were extracted from CAR T cells using radioimmunoprecipitation assay (RIPA) buffer (Thermo Fisher Scientific) containing protease inhibitor (Roche). Total protein concentration was determined using Pierce BCA assay (Thermo Fisher Scientific). Samples were separated by SDS–polyacrylamide gel electrophoresis, and separated proteins were transferred to nitrocellulose membranes using an iBlot2 transfer system (Thermo Fisher Scientific). Membranes were blocked with 5% nonfat milk–tris-buffered saline and incubated with primary antibodies against CD19 or β-actin. Membranes were washed and developed using species-specific secondary anti-IgG/horseradish peroxidase antibodies (R&D Systems) and Western Lightning Plus-ECL solution (PerkinElmer). Bands were visualized and quantified on an iBright 1500 imaging system (Thermo Fisher Scientific).

In vivo cystatin A model of CAR T cell expansion

6–8-week-old male NRG mice (Jackson Laboratory) were irradiated with a sublethal dose of 200 cGy (Day -1). The next day (Day 0), mice were injected with 4 x 10^5 NALM6 tumor cells via tail vein injection. On Day 4, mice were injected with 1 x 10^6 FMC63 CAR T cells ± Cystatin A overexpression or CAR T cells lacking a binding domain (ΔscFv) via tail vein injection. Animals were weighed twice weekly and monitored for signs of distress in accordance with institutional regulations. On day 28, animals were euthanized and tissues collected for analysis by flow cytometry.

Statistical Analysis

The respective statistical tests are stated in the figure legends. Generally, statistical significance between two groups was determined by two-sided Student's *t*-test or Mann-Whitney U test. Statistical significance between groups of three or more was determined

by one- or two-way analysis of variance (ANOVA). Significance of differences between cell numbers, mean fluorescence intensity, and area under curve, was calculated by two-sided Student's *t* test. Significance of differences in murine tumor control was determined by two-way ANOVA. All statistical tests were performed using Prism 10 (GraphPad). Results were considered significant when $p < 0.05$.

ACKNOWLEDGMENTS

The authors thank the Flow Cytometry Shared Service of the University of Maryland Marlene and Stewart Greenebaum Comprehensive Cancer Center for help with sorting cells and panel design. Research reported in this publication utilized the Preclinical Research Shared Resource at Huntsman Cancer Institute at the University of Utah and was supported by the National Cancer Institute of the National Institutes of Health under Award Number P30CA042014. This work was supported by funds through the Maryland Department of Health's Cigarette Restitution Fund Program (CH-649-CRF), the National Cancer Institute Cancer Center Support Grant (P30CA134274), the National Institutes of Health to AU (R35 GM145313), and by an NIAID-funded predoctoral fellowship to JMB (T32 AI095190). The plasmid pHIV-Luc-ZsGreen was a gift from Dr. B. Welm (Addgene #39196). The plasmid SFG.CNb30_opt.IRES.eGFP was a gift from Dr. M. Pule (Addgene #22493). The content is solely the responsibility of the authors and does not necessarily represent the official views of the NIH.

AUTHOR CONTRIBUTIONS

KAD and TL conceived the project, planned and performed experiments, analyzed data, and wrote the manuscript. KAD performed the majority of the described in vitro experiments, generated all transgenic T cells, developed the CompLuc assay, identified and validated the role of CTSB in CMT, and developed the CSTA-based approach of CMT inhibition in CAR T cells. KN and AP performed confocal microscopy and fixed coculture staining and imaging. JMB planned experiments, analyzed data, and edited the manuscript. EG performed CAR T cell phenotyping and analyzed data. FF wrote analysis scripts for CTSB dispersion. WS, ER, and DL planned and performed in vivo

models and analyzed data. XF developed full-spectrum flow cytometry panel and performed flow cytometry analysis. AW planned experiments and analyzed data. DA supervised CAR T cell phenotyping. AU planned and supervised microscopy experiments and analyzed data. TL supervised all work related to this project. All authors reviewed and approved the manuscript.

REFERENCES

1. Sadelain, M. CD19 CAR T Cells. *Cell* **171**, 1471 (2017).

2. Maude, S. L. *et al.* Tisagenlecleucel in Children and Young Adults with B-Cell Lymphoblastic Leukemia. *N. Engl. J. Med.* **378**, 439–448 (2018).

3. Sadelain, M., Rivière, I. & Riddell, S. Therapeutic T cell engineering. *Nature* **545**, 423–431 (2017).

4. Raje, N. *et al.* Anti-BCMA CAR T-Cell Therapy bb2121 in Relapsed or Refractory Multiple Myeloma. *N. Engl. J. Med.* **380**, 1726–1737 (2019).

5. D'Agostino, M. & Raje, N. Anti-BCMA CAR T-cell therapy in multiple myeloma: can we do better? *Leukemia* **34**, 21–34 (2020).

6. Romanski, A. *et al.* CD19-CAR engineered NK-92 cells are sufficient to overcome NK cell resistance in B-cell malignancies. *J. Cell. Mol. Med.* **20**, 1287–1294 (2016).

7. Boissel, L. *et al.* Retargeting NK-92 cells by means of CD19- and CD20-specific chimeric antigen receptors compares favorably with antibody-dependent cellular cytotoxicity. *OncoImmunology* **2**, e26527 (2013).

8. Hamieh, M. *et al.* CAR T cell trogocytosis and cooperative killing regulate tumour antigen escape. *Nature* **568**, 112–116 (2019).

9. Olson, M. L. *et al.* Low-affinity CAR T cells exhibit reduced trogocytosis, preventing rapid antigen loss, and increasing CAR T cell expansion. *Leukemia* **36**, 1943–1946 (2022).

10. Li, Y. *et al.* KIR-based inhibitory CARs overcome CAR-NK cell trogocytosis-mediated fratricide and tumor escape. *Nat Med* **28**, 2133–2144 (2022).

11. Camviel, N. *et al.* Both APRIL and antibody-fragment-based CAR T cells for myeloma induce BCMA downmodulation by trogocytosis and internalization. *J. Immunother. Cancer* **10**, e005091 (2022).

12. Cohen, A. D. *et al.* B cell maturation antigen-specific CAR T cells are clinically active in multiple myeloma. *J. Clin. Investig.* **129**, 2210–2221 (2019).

13. Radhakrishnan, S. V. *et al.* CD229 CAR T cells eliminate multiple myeloma and tumor propagating cells without fratricide. *Nat. Commun.* **11**, 798 (2020).

14. Marei, H. *et al.* Antibody targeting of E3 ubiquitin ligases for receptor degradation. *Nature* **610**, 182–189 (2022).

15. Békés, M., Langley, D. R. & Crews, C. M. PROTAC targeted protein degraders: the past is prologue. *Nat. Rev. Drug Discov.* **21**, 181–200 (2022).

16. Brooks, S. R., Kirkham, P. M., Freeberg, L. & Carter, R. H. Binding of Cytoplasmic Proteins to the CD19 Intracellular Domain Is High Affinity, Competitive, and Multimeric. *J. Immunol.* **172**, 7556–7564 (2004).

17. Ruella, M. *et al.* Induction of resistance to chimeric antigen receptor T cell therapy by transduction of a single leukemic B cell. *Nat. Med.* **24**, 1499–1503 (2018).

18. Dixon, A. S. *et al.* NanoLuc Complementation Reporter Optimized for Accurate Measurement of Protein Interactions in Cells. *ACS Chem. Biol.* **11**, 400–408 (2016).

19. Miyake, K. *et al.* Trogocytosis of peptide-MHC class II complexes from dendritic cells confers antigen-presenting ability on basophils. *Proc Natl Acad Sci U S A* **114**, 1111–1116 (2017).

20. Gilmartin, A. A., Ralston, K. S. & Petri, W. A. Inhibition of Amebic Cysteine Proteases Blocks Amebic Trogocytosis but Not Phagocytosis. *J. Infect. Dis.* **221**, 1734–1739 (2020).

21. Reed, J., Reichelt, M. & Wetzel, S. A. Lymphocytes and Trogocytosis-Mediated Signaling. *Cells* **10**, 1478 (2021).

22. Hudrisier, D., Aucher, A., Puaux, A.-L., Bordier, C. & Joly, E. Capture of Target Cell Membrane Components via Trogocytosis Is Triggered by a Selected Set of Surface Molecules on T or B Cells. *J. Immunol.* **178**, 3637–3647 (2007).

23. Cavallo-Medved, D., Moin, K. & Sloane, B. Cathepsin B. *AFCS Nat Mol Pages* **2011**, A000508 (2011).

24. Mort, J. S. & Buttle, D. J. Cathepsin B. *Int. J. Biochem. Cell Biol.* **29**, 715–720 (1997).

25. Vidak, E., Javoršek, U., Vizovišek, M. & Turk, B. Cysteine Cathepsins and Their Extracellular Roles: Shaping the Microenvironment. *Cells* **8**, 264 (2019).

26. Balaji, K. N., Schaschke, N., Machleidt, W., Catalfamo, M. & Henkart, P. A. Surface Cathepsin B Protects Cytotoxic Lymphocytes from Self-destruction after Degranulation. *Journal of Experimental Medicine* **196**, 493–503 (2002).

27. Olson, O. C. & Joyce, J. A. Cysteine cathepsin proteases: regulators of cancer progression and therapeutic response. *Nat Rev Cancer* **15**, 712–729 (2015).

28. Gabrijelcic, D. *et al.* Cathepsins B, H and L in human breast carcinoma. *Eur J Clin Chem Clin Biochem* **30**, 69–74 (1992).

29. Estrada, S. *et al.* The Role of Gly-4 of Human Cystatin A (Stefin A) in the Binding of Target Proteinases. Characterization by Kinetic and Equilibrium Methods of the Interactions of Cystatin A Gly-4 Mutants with Papain, Cathepsin B, and Cathepsin L. *Biochemistry* **37**, 7551–7560 (1998).

30. Pavlova, A., Krupa, J. C., Mort, J. S., Abrahamson, M. & Björk, I. Cystatin inhibition of cathepsin B requires dislocation of the proteinase occluding loop. Demonstration by release of loop anchoring through mutation of His110. *FEBS Lett.* **487**, 156–160 (2000).

31. Pavlova, A. & Björk, I. Grafting of Features of Cystatins C or B into the N-Terminal Region or Second Binding Loop of Cystatin A (Stefin A) Substantially Enhances Inhibition of Cysteine Proteinases. *Biochemistry* **42**, 11326–11333 (2003).

32. Jenko, S. *et al.* Different propensity to form amyloid fibrils by two homologous proteins—Human stefins A and B: Searching for an explanation. *Proteins: Struct., Funct., Bioinform.* **55**, 417–425 (2004).

33. Grover, P. *et al.* Chimeric antigen receptor T-cell therapy in adults with B-cell acute lymphoblastic leukemia. *Blood Adv* **6**, 1608–1618 (2022).

34. Xu, X. *et al.* Mechanisms of Relapse After CD19 CAR T-Cell Therapy for Acute Lymphoblastic Leukemia and Its Prevention and Treatment Strategies. *Front. Immunol.* **10**, 2664 (2019).

35. Gu, T., Zhu, M., Huang, H. & Hu, Y. Relapse after CAR-T cell therapy in B-cell malignancies: challenges and future approaches. *J. Zhejiang Univ.-Sci. B* **23**, 793–811 (2022).

36. Ruella, M. *et al.* Induction of resistance to chimeric antigen receptor T cell therapy by transduction of a single leukemic B cell. *Nat. Med.* **24**, 1499–1503 (2018).

37. Towatari, T. *et al.* Novel epoxysuccinyl peptides A selective inhibitor of cathepsin B, in vivo. *FEBS Lett.* **280**, 311–315 (1991).

38. Murata, M. *et al.* Novel epoxysuccinyl peptides Selective inhibitors of cathepsin B, in vitro. *FEBS Lett.* **280**, 307–310 (1991).

39. Newick, K., O'Brien, S., Moon, E. & Albelda, S. M. CAR T Cell Therapy for Solid Tumors. *Annu. Rev. Med.* **68**, 139–152 (2016).

40. Sterner, R. C. & Sterner, R. M. CAR-T cell therapy: current limitations and potential strategies. *Blood Cancer J.* **11**, 1–11 (2021).

41. Mause, E. R. V. *et al.* Systematic single amino acid affinity tuning of CD229 CAR T cells retains efficacy against multiple myeloma and eliminates on-target off-tumor toxicity. *Sci. Transl. Med.* **15,** eadd7900 (2023).

42. Lee, D. W. *et al.* T cells expressing CD19 chimeric antigen receptors for acute lymphoblastic leukaemia in children and young adults: a phase 1 dose-escalation trial. *Lancet* **385,** 517–528 (2015).

43. Veatch, S. L. *et al.* Correlation Functions Quantify Super-Resolution Images and Estimate Apparent Clustering Due to Over-Counting. *PLoS ONE* **7,** e31457 (2012).